

Strongly disordered Hubbard model in one dimension: Spin and orbital infinite randomness and Griffiths phases

R. Mélin

Centre de Recherches sur les Très Basses Températures (CRTBT), CNRS, Boite Postale 166, F-38042 Grenoble, France

F. Iglói

*Research Institute for Solid State Physics and Optics, H-1525 Budapest, P.O. Box 49, Hungary and**Institute of Theoretical Physics, Szeged University, H-6720 Szeged, Hungary*

(Received 11 July 2006; published 4 October 2006)

We study by the strong disorder renormalization group (RG) method the low-energy properties of the one-dimensional Hubbard model with random-hopping matrix-elements $t_{min} < t < t_{max}$, and with random onsite Coulomb repulsion terms $0 \leq U_{min} < U < U_{max}$. There are two critical phases, corresponding to an infinite randomness spin random singlet for strong interactions ($U_{min} > t_{max}$) and to an orbital infinite randomness fixed point for vanishing interactions ($U_{max}/t_{max} \rightarrow 0$). To each critical infinite randomness fixed point is connected a Griffiths phase, the correlation length, and dynamical exponent of which have well defined asymptotic dependences on the corresponding quantum control parameter. The theoretical predictions for the scaling in the vicinity of the critical points compare well to numerical RG simulations.

DOI: [10.1103/PhysRevB.74.155104](https://doi.org/10.1103/PhysRevB.74.155104)

PACS number(s): 75.10.Nr, 75.50.Lk, 64.60.Ak

I. INTRODUCTION

The Hubbard model is one of the simplest quantum many-body models of interacting fermions. Detailed exact information in one-dimension (1D) for the pure model is provided by Bethe ansatz,¹ bosonization,² and by factorizing the wave function.³ For repulsive interaction $U > 0$, the 1D model is the simplest system with a Mott transition at half-filling, having a finite charge gap $\Delta_c > 0$. At the same time the spin gap Δ_s is vanishing, and the spin-spin correlation function has quasi-long-range order.

Quenched, i.e., time-independent disorder is an unavoidable feature of real materials and there are quasi-1D systems, such as tetracyanoquinodimethan (TCNQ) compounds⁴ for which the Hubbard model with random parameters is conjectured to be relevant. Earlier theoretical studies^{5–7} based on the real-space renormalization group (RG) method,⁵ quantum Monte Carlo (QMC) simulations,⁶ and density matrix renormalization (DMRG)⁷ are primarily interested in the effect of weak random potentials of strength ϵ , in order to understand the metal-insulator transition in the presence of interactions. Repulsive interactions turn out to contrast with attractive interactions: like the noninteracting model,⁸ the system with repulsive interactions is in the insulating phase⁹ whereas a metal-insulator transition is predicted for strong enough attractive interaction. For repulsive interactions, the charge gap is reduced by the random potential and for strong enough ϵ there is a transition from a Mott insulator (in which the charge gap is finite and the spin-spin correlation length is infinite) to an Anderson insulator (with a vanishing charge gap and a finite spin-spin correlation length).

Other investigations^{10,11} of insulating disordered 1D systems, motivated by the understanding of the N-methylphenazinium (NMP)-TCNQ compound,¹⁰ and more recently¹¹ by the inorganic spin-Peierls compound CuGeO_3 , have relied on the evaluation of the uniform paramagnetic susceptibility within strong disorder. The proposed effective

model⁴ is a random exchange $S=1/2$ antiferromagnetic Heisenberg spin chain. The RG introduced by Ma, Dasgupta, and Hu^{12,13} to study this model was first implemented numerically,¹² and then analytically by Fisher.¹⁴ According to the RG results, the ground state consists of a collection of randomly distributed singlets. Disorder grows without limit as the energy is reduced. The resulting singular behavior is typical of an “infinite randomness” fixed point: the low-temperature uniform susceptibility diverges as (Ref. 14) follows:

$$\chi(T) \sim \frac{1}{T |\ln T|^2} \quad (1)$$

which has been found first in numerical RG studies.¹⁵ On the other hand the experimentally measured susceptibility in TCNQ materials is accurately described by (Ref. 10)

$$\chi(T) \sim \frac{1}{T^\beta}, \quad (2)$$

with $\beta \approx 0.55 - 0.9$. The results of QMC simulations⁶ are in qualitative agreement with the power-law behavior in Eq. (2). A similar behavior was found more recently in the insulator $o\text{-TaS}_3$ where the power-law behavior in the susceptibility accurately matches¹⁶ both the power-law specific heat and the power-law electronic spin resonance spectroscopy signal.¹⁷

It is of importance to understand the low-energy properties of the Hubbard model in the presence of different types of randomness and arbitrary interactions. As shown in Ref. 18, dilute impurities in an interacting quasi-1D conductor can stabilize a “bounded” Luttinger liquid on ballistic finite size segments in between two impurities that constitute infinite barriers at low energy.¹⁹ We consider in the following a similar problem in the commensurate case and in the regime of strong disorder, likely to be relevant to a finite concentration of impurities. The combined effects of disorder in the

hopping matrix element and in the interaction result in spin and orbital random singlets, and spin and orbital Griffiths phases. The transitions and crossovers between them is the subject of our paper. For completeness we also consider the possibility of diagonal disorder in the form of a random potential, giving rise to an Anderson insulator.

The structure of the paper is as follows. The random Hubbard model is introduced in Sec. II. The basic steps of the strong disorder RG method, together with the overall phase diagram of the model, are presented in Sec. III. Results of numerical renormalization group calculations are given in Sec. IV and discussed in Sec. V.

II. MODEL

We start with the Hamiltonian of the 1D Hubbard model:

$$\mathcal{H} = - \sum_{i=1}^L \sum_{\sigma=\uparrow,\downarrow} t_i (c_{i,\sigma}^+ c_{i+1,\sigma} + c_{i+1,\sigma}^+ c_{i,\sigma}) + \sum_i U_i n_{i,\uparrow} n_{i,\downarrow} + \sum_{i,\sigma} \epsilon_i c_{i,\sigma}^+ c_{i,\sigma} + \mathcal{H}' \quad (3)$$

in which the extra term \mathcal{H}' is generated during renormalization, so that $\mathcal{H}'=0$ in the initial condition of the physical model. The operators $c_{i,\sigma}^+$ and $c_{i,\sigma}$ create and annihilate a spin- σ fermion at site $i=1, 2, \dots, L$, and $n_{i,\sigma} = c_{i,\sigma}^+ c_{i,\sigma}$. We restrict ourselves to repulsive onsite Coulomb interactions being independent random numbers such that $0 \leq U_{\min} < U_i < U_{\max}$, chosen in the distribution

$$\mathcal{P}(U) = \mathcal{F}_\alpha(U, U_{\min}, U_{\max}) \equiv \alpha \frac{(U_{\max} - U_{\min})^{-\alpha}}{(U - U_{\min})^{1-\alpha}}. \quad (4)$$

Similarly, the exchange integrals $t_{\min} < t_i < t_{\max}$ are independent and identically distributed random numbers, and we consider the distribution $\mathcal{P}(t) = \mathcal{F}_\alpha(t, t_{\min}, t_{\max})$. We have also included in the Hamiltonian in Eq. (3) a symmetrically distributed random potential, $-\epsilon_{\max} < \epsilon < \epsilon_{\max}$. The absolute value $|\epsilon|$ of the diagonal disorder potential is drawn in the distribution $\mathcal{P}(|\epsilon|) = \mathcal{F}_\alpha(|\epsilon|, 0, \epsilon_{\max})$. We use the same exponent, $\alpha = \alpha_t = \alpha_\epsilon = \alpha_U$ for the hopping, diagonal disorder potential, and interaction distributions. The parameter $\alpha^{-2} = \text{var}[\ln U] = \text{var}[\ln t] = \text{var}[\ln |\epsilon|]$ measures the strength of disorder for $U_{\min} = t_{\min} = 0$, ($\text{var}[x]$ stands for the variance of x). A uniform distribution corresponds to $\alpha=1$. We restrict ourselves to the half-filled case: $\sum_i \sum_\sigma n_{i,\sigma} = L$.

III. STRONG DISORDER RG, AND OVERALL PHASE DIAGRAM

To analyze the low-energy properties of the 1D random Hubbard model we use the strong disorder RG method,¹³ (for the random bosonic Hubbard chain, see²⁰) in which the interaction term (being the onsite Coulomb interaction, the hopping integral or the onsite potential) with the largest parameter in the Hamiltonian in Eq. (3), that defines the energy scale Ω . The largest coupling with strength Ω is eliminated, which results in renormalized parameters between the remaining degrees of freedom, that are calculated in perturba-

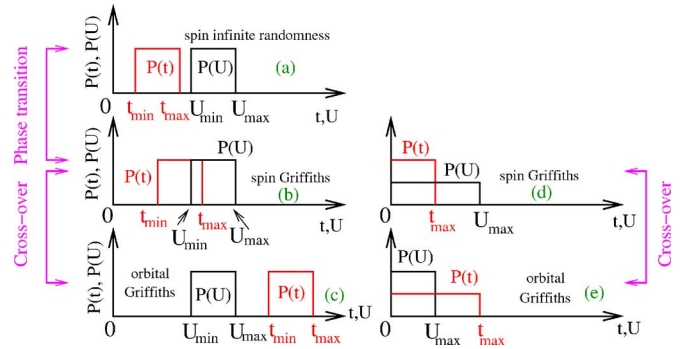


FIG. 1. (Color online) Schematic representation of the different hopping and onsite interaction energy distributions (drawn for $\alpha = 1$), the corresponding phases and the transition or crossover between them.

tion. We first set $\epsilon_{\max}=0$ and thus omit the random potential.

A. Interaction dominated region

We start with a disorder in which the interaction plays the dominant role, so that even the smallest interaction is larger than the possible maximal value of the hopping integral [see Fig. 1(a)]:

$$U_{\min} > t_{\max}. \quad (5)$$

In this case only interactions are decimated out in the first stage of the RG, corresponding to U transformations.

1. U transformation

Let us consider the first decimation steps, when the largest interaction term is, say, $U_2 = \Omega$, the hopping integral between sites 1 and 2 is denoted by t_1 , and it is denoted by t_2 between sites 2 and 3. The double occupancy of site 2 is forbidden [at least up to order of $O(\max(t_1, t_2)/U_2)$] because of the large value of U_2 . The Hamiltonian is then projected on the subspace without double occupancy. A virtual exchange interaction is then generated between the spin at site 2 and between the neighboring sites. If site 1 contains two fermions the exchange interaction is given in a second-order perturbation calculation as follows:

$$\mathcal{H}'_1 = \sum_{\mathbf{S}_1} \tilde{J}_1 \mathbf{S}_1 \cdot \mathbf{S}_2, \quad \tilde{J}_1 \approx \frac{2t_1^2}{U_2}, \quad (6)$$

and similarly between sites 2 and 3. New antiferromagnetic Heisenberg exchange interactions are thus generated during renormalization. All the interactions are first decimated out with the condition in Eq. (5). If we perform the U transformation at both ends of a link we obtain for the final exchange term: $\tilde{J}_1 \approx 2t_1^2/U_2 + 2t_1^2/U_1$ and in \mathcal{H}'_1 in Eq. (6) there is no sum over \mathbf{S}_1 , since double occupancy of site 1 is also forbidden. Thus after eliminating all the onsite Coulomb interactions we are left with the Hamiltonian of the random antiferromagnetic Heisenberg chain: $\mathcal{H}' = \sum_{i=1}^L J_i \mathbf{S}_i \cdot \mathbf{S}_{i+1}$. This model has been thoroughly studied by strong disorder RG (Ref. 14). The corresponding RG step is called a J transformation.

2. J transformation

In the decimation procedure the two spins coupled by the strongest exchange coupling, say with $J_2=\Omega$, form a singlet and are eliminated, while between the remaining sites, 1 and 4, a renormalized exchange coupling is generated, given by $\tilde{J} \approx J_1 J_3 / 2J_2$, where J_1 and J_3 are the original couplings joining to J_2 .

3. Random singlet spin infinite randomness phase

The coupling distribution broadens without limit as the renormalization goes on and the energy scale is lowered, corresponding to a spin infinite randomness fixed point for the distributions in Fig. 1(a). At this fixed point, the length-scale L and the energy scale Δ (the smallest gap) are related by

$$-\ln \Delta \sim L^{1/2}, \quad (7)$$

and the distribution function $P_L(\Delta)$ scales as follows:

$$\ln[L^{1/2}P_L(\Delta)] \approx f(L^{-1/2} \ln \Delta). \quad (8)$$

The ground state is the so-called random singlet phase, consisting of effective singlets between sites arbitrarily far apart. The average spin-spin correlation function decays as $C(r) \sim r^{-2}$. The low-temperature susceptibility has a Curie-like form with logarithmic corrections, as given in Eq. (1). The predictions of the asymptotically exact RG²¹ have been confirmed by numerical simulations,^{22,23} see however, Ref. 24.

4. Random dimer phase

To introduce the notion of Griffiths phase²⁵ that will be useful for discussing the random Hubbard model, we consider now an enforced dimerization, with the couplings J_o at odd positions, and J_e at even positions taken from different distributions. The control parameter δ_{dim} is defined as $\delta_{dim} = [\ln J_o]_{av} - [\ln J_e]_{av}$, where $[\dots]_{av}$ stands for an average over quenched disorder. This type of model is obtained through renormalization of the random Hubbard model if the hopping terms and/or the interactions in Eq. (3) are dimerized and if the relation in Eq. (5) is satisfied. The dimerized (nonrandom) Hubbard model is used to describe the low-energy properties of Bechgaard salts²⁶ and other quasi-1D systems.²⁷

The dimerized random Heisenberg chain is renormalized to a zero energy fixed point,^{14,28} with short range spatial correlations, i.e., the correlation length is $\xi < \infty$. This is the so-called random dimer phase, being a Griffiths phase consisting of long singlet bonds involving the J_o couplings and short singlet bonds involving the J_e couplings. The average size ξ of the latter is used to define the average correlation length, which behaves for small dimerization as such,

$$\xi \sim \delta_{dim}^{-2}. \quad (9)$$

On the other hand, the length of the long singlet bonds is proportional to the size L of the system, and the low-energy excitations goes to zero as follows:

$$\Delta \sim L^{-z}. \quad (10)$$

Here $z < \infty$ is the dynamical exponent which depends on the value of δ_{dim} , thus on the distribution of disorder. Close to the random singlet phase, $|\delta_{dim}| \ll 1$, the dynamical exponent diverges as follows:

$$z \sim \delta_{dim}^{-1}. \quad (11)$$

If the low-energy excitations are localized, which is the case in the random dimer phase, the gap distribution $P_L(\Delta)$ scales as follows:

$$P_L(\Delta) = L^z g(L^z \Delta) \sim \Delta^{-1+1/z}. \quad (12)$$

The low-temperature uniform susceptibility in the random dimer phase behaves like $\chi(T) \sim 1/T^{1-1/z}$, which is in the same form as the experimental result in Eq. (2), with $\beta=1-1/z$. In the random singlet phase, Eqs. (10) and (12) are replaced by Eqs. (7) and (8), respectively.

B. Hopping dominated region

Some hopping matrix elements are also decimated as Ω is lowered below t_{max} , if the condition set by Eq. (5) on the strength of the onsite Coulomb interaction is not satisfied, which we consider now.

1. t transformation

If the energy Ω corresponds to a hopping term, say $\Omega = t_2$, then two fermions (one with $\sigma=\uparrow$ and the other with $\sigma=\downarrow$) are localized on the bond between sites 2 and 3, and these sites are eliminated. A small hopping term is generated between the remaining sites 1 and 4, which is given in second order perturbation by $\tilde{t} \approx -t_1 t_3 / t_2$. This transformation has an effect on the value of the interaction term, say at site 1, provided U_1 has not yet been decimated out. For its renormalized value we obtain:

$$\tilde{U}_1 \approx U_1 - \frac{t_1 t_3}{t_2}. \quad (13)$$

Similarly the random potential at site 1 is modified and transformed as written

$$\tilde{\epsilon}_1 \approx \epsilon_1 + \frac{t_1 t_3}{t_2}. \quad (14)$$

Formula analogous to Eqs. (13) and (14) hold also at site 4.

Finally, if two J couplings (denoted by J_1 and J_3) have already been generated at sites 1 and 4, an effective exchange interaction is also generated between sites 1 and 4:

$$\tilde{J} \approx \frac{J_1 J_3}{16|t_2|}. \quad (15)$$

However, if $J_1=0$ and/or $J_3=0$ we obtain to third order:

$$\tilde{J} = 12 \frac{|t_1|^2 |t_3|^2}{|t_2|^3}. \quad (16)$$

The t transformation has an influence on the renormalized value of the other parameters, in particular on the onsite

Coulomb interaction. In particular, both t and U transformations are generated at some stage of the renormalization for any finite value of $U_{max} > 0$.

2. Orbital infinite randomness fixed point: $U_{max} = \epsilon_{max} = 0$

The problem reduces to the random tight-binding model and the RG process involves solely t transformations if $U_{max} = 0$ (and $\epsilon_{max} = 0$). The fixed point of the RG is now an orbital infinite randomness fixed point,^{29,30} which is isomorph to the fixed point of the random antiferromagnetic Heisenberg chain, as discussed in Sec. III A 3. In particular the relations in Eqs. (7) and (8) remain valid. The ground state of the system is made of t -frozen pairs of fermions, where the length of a pair can be arbitrarily large.

C. Interplay between interaction and hopping

In the general situation $U_{min} < t_{max}$, $U_{max} > 0$ where the t and U distributions overlap [this corresponds to Figs. 1(b)–1(e)], both U and t terms are decimated during renormalization and J transformations are also carried out. The ground state of the system is a mixture of J singlets and frozen t pairs and the average size ξ_J of the singlets, and that ξ_t of the t pairs are finite. The largest of the two defines the correlation length. At the same time the energy scale decreases to zero with the size of the system as in Eq. (10). We are thus in a Griffiths phase, analogous to the random dimer phase described in Sec. III A 4, which can be divided in two regions. The onsite Coulomb interaction plays the dominant role in the “spin Griffiths phase” corresponding to $\xi_J > \xi_t$ for the coupling distributions in Figs. 1(b) and 1(d), whereas hopping is dominant in the “orbital Griffiths phase,” corresponding to $\xi_t > \xi_J$ for the coupling distributions in Figs. 1(c) and 1(e). There is a crossover, but no sharp transition in between these two Griffiths phases, similar to that observed in other random quantum models, such as the random dimerized $S=1$ chain³¹ or random Heisenberg ladders.³² In the following subsections we analyze the properties of the Griffiths phases in the vicinity of the infinite randomness fixed points. Numerical results far from the random critical points are presented afterwards.

1. Spin Griffiths phase: $0 < t_{max} - U_{min} \ll U_{max}$

Let us start to analyze the properties of the system in the vicinity of the random singlet fixed point, when $0 < t_{max} - U_{min} \ll U_{max}$. We define the control-parameter δ_U as the fraction of nondecimated U terms at $\Omega = t_{max}$:

$$\delta_U = \int_{U_{min}}^{t_{max}} P(U) dU = \left(\frac{t_{max} - U_{min}}{U_{max} - U_{min}} \right)^\alpha. \quad (17)$$

Here the second relation holds for the power-law distribution in Eq. (4).

As we discussed in Sec. III B, some t terms are also decimated out as Ω is lowered below t_{max} , and the density ρ_t of the frozen t terms is given by $\rho_t \sim \delta_U$. The typical length scale in the system is given by the typical distance between two frozen t terms, and is thus

$$\xi_{typ} \sim 1/\rho_t \sim \delta_U^{-1}. \quad (18)$$

On the other hand the average correlation length is given by the average distance between spins forming a singlet through a J coupling. In the random singlet phase, i.e., for $\delta_U = 0$, the singlets are formed from either odd or even bonds. For $\delta > 0$ the correlated segments are broken if two neighboring t terms are frozen, which leads to a change of the parity of the singlets, see the discussion in Sec. III A 4. Thus we obtain for the average correlation length

$$\xi \sim 1/\rho_t^2 \sim \delta_U^{-2}. \quad (19)$$

Finally, one considers the typical value of the gap, which is related to the value of the gap in the random singlet phase of size $\sim \xi$. Equations (7), (10), and (19) lead to

$$z \sim \delta_U^{-1}. \quad (20)$$

Now comparing Eqs. (19) and (20) with those of Eqs. (9) and (11) in the random dimer phase we conclude that δ_U in Eq. (17) plays the role of the control parameter in the spin Griffiths phase.

2. Orbital Griffiths phase— $0 < U_{max} \ll t_{max}$

Second, we consider the behavior of the system in the vicinity of the orbital infinite randomness fixed point, $0 < U_{max} \ll t_{max}$. In the initial steps of the renormalization solely t terms are decimated out, until the energy scale is lowered below $\sim U_{max}$, when also U terms are eliminated. The density of decimated U sites is given by $\rho_U \sim |\ln U_{max}|^{-2}$, which follows from Eq. (7), with the correspondences $\Delta \sim U_{max}$ and $L \sim \rho_U^{-1}$. We have thus for the correlation length ξ_t (the average size of the t singlets): $\xi_t \sim \rho_U^{-1} \sim |\ln U_{max}|^2$. Comparing to Eq. (9) in the random dimer phase we identify the control parameter in the orbital Griffiths phase as follows:

$$\delta_t = |\ln(U_{max}/t_{max})|^{-1}. \quad (21)$$

Repeating the arguments used in the vicinity of the random singlet phase we obtain that the relations in Eqs. (18)–(20) remain valid by simply replacing δ_U by δ_t .

D. Role of the random potential—Anderson vs Mott insulator phases

In order to determine the overall phase diagram of the random Hubbard model we consider also the role of the random potential $\{\epsilon_j\}$ which plays a special role in the renormalization in 1D. If at some stage of the renormalization one random potential term is decimated, say $\epsilon_2 = \Omega$, then two fermions are frozen at site 2, and this site is eliminated. This transformation does not influence the value of the parameters at the neighboring sites because no hopping is generated between the remaining sites 1 and 3. Transport is thus blocked at this site. The random potentials are just slightly modified by other t transformations [see Eq. (14)]. The random potentials are thus also decimated at some stage of the RG if $\epsilon_{max} > U_{max} \geq 0$. As a consequence a finite fraction of sites are frozen and the system scales into the Anderson insulator

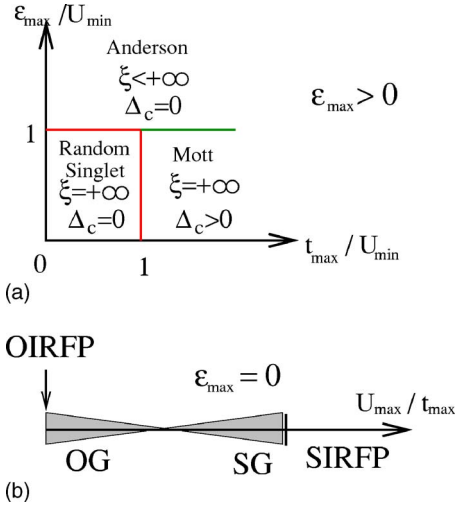


FIG. 2. (Color online) Schematic phase diagram of the random Hubbard chain. (a) Including a random potential and with weak disorder in U and t . (b) Without random potential and with strong disorder in U and t . This latter corresponds to the numerical work in the paper. OIRFP stands for orbital infinite randomness, OG for orbital Griffiths [for the distributions in Fig. 1(c)], SG for spin Griffiths [for the distributions in Fig. 1(b)], SID for spin infinite randomness [for the distributions in Fig. 1(a)]. See the text for the properties of the different phases. We suppose as in Fig. 1 coupling distributions with constant values of $U_{max}-U_{min}$ and $t_{max}-t_{min}$ while U_{max} and t_{max} are varying.

phase. In the other limiting case, $\epsilon_{max} < U_{min}$, the behavior of the system is dominated by the onsite Coulomb repulsion, thus no fermions are frozen due to the random potential and the system scales into the Mott insulator phase.

E. Phase diagram

We conclude this section by presenting the phase diagram of the random Hubbard model in 1D, which constitutes the main result of this paper. First we consider in Fig. 2(a) the effect of a random potential, when the disorder in the other terms is weak, so that $(t_{max}-t_{min})/(t_{max}+t_{min}) \sim (U_{max}-U_{min})/(U_{max}+U_{min}) = D_{t,U} \ll \epsilon_{max}$. Previous numerical work^{6,7} considered nonrandom U and t , thus $D_{t,U}=0$. Here we extend these results to weak disorder. The random potential plays a dominant role for $\epsilon_{max}/U_{min} > 1$, when the system is in the Anderson insulator phase, with a finite spin-spin correlation length $\xi < \infty$ and with a vanishing charge gap $\Delta_c=0$. If $D_{t,U}=0$ and $\epsilon_{max}/U_{min} < 1$ the system is in the Mott insulator phase, $\xi=\infty$ but with $\Delta_c > 0$. We expect this scenario to remain valid even for weak disorder ($D_{t,U} \ll \epsilon_{max}$) provided hopping dominates over Coulomb repulsion, thus $t_{max}/U_{min} > 1$. If, however, the onsite Coulomb repulsion is sufficiently strong ($\epsilon_{max}/U_{min} < 1$ and $t_{max}/U_{min} < 1$) the system is in the spin random singlet phase, see Sec. III A 3, with a divergent spin-spin correlation length, $\xi=\infty$ and with a vanishing charge gap, $\Delta_c=0$. Transition between the Mott and the Anderson phases is found to be controlled by a conventional random fixed point,^{6,7} whereas transitions from the spin random singlet phase are likely of an infinite randomness type.

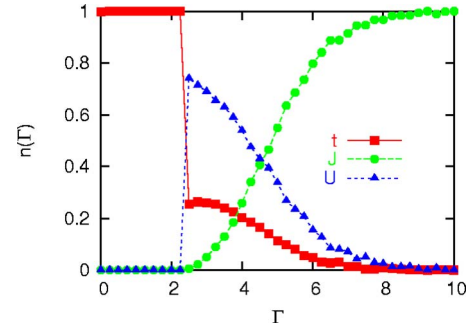


FIG. 3. (Color online) The fractions of different RG transformations as a function of the logarithm-energy scale, $\Gamma = -\ln \Omega$, for the random 1D chain.

In Fig. 2(b) we present the phase diagram without a random potential, $\epsilon_{max}=0$, but for sufficiently strong disorder in U and t as a function of $r=U_{max}/t_{max}$. For $U_{max}/t_{max}=0$ the system is in the orbital infinite randomness fixed point, the properties of which are described in Sec. III B 2. In the other limiting case with $U_{min} > t_{max}$, which corresponds to $U_{max}/t_{max} > r_c > 0$, the system is in the spin random singlet phase (see Sec. III A 3). For $0 < U_{max}/t_{max} < r_c$ the system is in the Griffiths phase, which is divided in an orbital Griffiths phase (Sec. III C 2) for $0 < U_{max}/t_{max} \ll r_c$, and in a spin Griffiths phase (Sec. III C 1) for $0 \ll U_{max}/t_{max} < r_c$. In the following section we now study numerically the properties of the phase diagram in Fig. 2(b).

IV. NUMERICAL RESULTS

We consider typically 250 000 independent random samples taken from the distribution in Eq. (4) to evaluate the dynamical exponent in the numerical implementation of the strong disorder RG method. We use smaller statistics of $\sim 10\,000$ samples for the evaluation of the correlation lengths. The numerical results are presented only for the uniform distribution with $\alpha=1$, but we obtained similar results for smaller values of α . The length of the chain is varied up to $L=2048$ and the decimation is performed up to the last remaining particle or spin singlet. The gap Δ at the last step of renormalization is identified as the gap of the random chain and we have also evaluated the length scales ξ_t and ξ_J from the density of the decimated t and J terms, respectively.

A. Qualitative features of the RG flow

To illustrate the behavior of the RG flow we have calculated the fraction $n_t(\Gamma)\delta\Gamma$ of t transformations, the fraction $n_U(\Gamma)\delta\Gamma$ of U transformations, and the fraction $n_J(\Gamma)\delta\Gamma$ of J transformations in an interval $[\Gamma, \Gamma + \delta\Gamma]$, where $\Gamma = -\ln \Omega$ is the logarithm-energy scale. The quantities are normalized in such a way as $n_t(\Gamma) + n_U(\Gamma) + n_J(\Gamma) = 1$.

The variations of $n_t(\Gamma)$, $n_U(\Gamma)$, $n_J(\Gamma)$ for the 1D chain are shown in Fig. 3 for $U_{max}=0.1$, $t_{max}=1$, and $\alpha=1$ with $U_{min}=t_{min}=0$. As seen in this figure only t terms are decimated out at the beginning of the RG, and the decimation of the U terms starts only when Ω is lowered below U_{max} . J terms are also generated through U decimations, which are then also

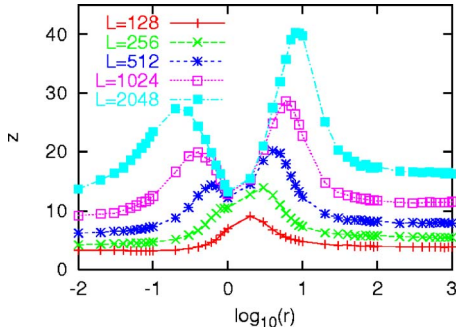


FIG. 4. (Color online) Dynamical exponent as a function of $r = U_{max}/t_{max}$ for different system sizes ($U_{min}=t_{min}=0$, $\alpha=1$).

decimated. The U and t terms gradually die out by further decreasing Ω and one is left with the J transformations at low energy.

B. Properties of the Griffiths phases

1. Dynamical exponent

The dynamical exponent z is determined from the distribution of the gaps, which in the Griffiths phases follows the scaling form given in Eq. (12). For a finite system this procedure results in effective L -dependent dynamical exponents, that are then extrapolated to $L=\infty$. The calculated effective dynamical exponents for the power-law distribution in Eq. (4) with $t_{min}=U_{min}=0$ and $\alpha=1$ for various values of $r = U_{max}/t_{max}$ are shown in Fig. 4. For these distributions the infinite randomness fixed points are located at $r=0$ (orbital infinite randomness fixed point), and at $r=\infty$ (spin random singlet, infinite randomness phase). The dynamical exponent z is formally infinite at both fixed points, which is compatible with the fact that the effective z is increasing with L with no sign of saturation. It is also interesting to note that the maxima of the effective exponent in the orbital Griffiths phase for a size L are approximately the same as the maxima of the same curve in the spin Griffiths phase, however, with a size $L/2$. This is because the spin Griffiths phase involves approximately the double number of RG steps (in the spin Griffiths phase one also makes a set of extra U transformations).

To have a qualitative analysis of the data we recall that close to the infinite randomness fixed points the effective exponent $z(\delta, L)$ obeys the scaling form:

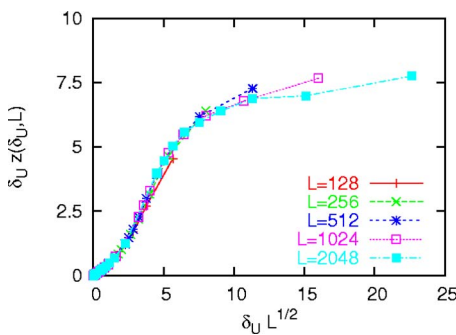


FIG. 5. (Color online) Scaling plot of the dynamical exponent in Fig. 4 in the spin Griffiths phase, with δ_U in Eq. (17).

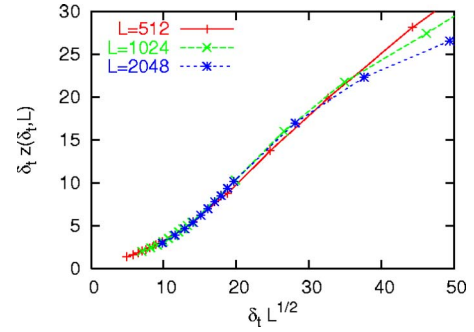


FIG. 6. (Color online) The same as in Fig. 5 in the orbital Griffiths phase, with δ_t in Eq. (21).

$$z(\delta, L) = \delta^{-1} \bar{z}(L^{1/2} \delta), \quad (22)$$

in which we have incorporated relations in Eq. (11) and in Eq. (9). Furthermore, the scaling function behaves like $\bar{z}(x) \sim x$ for small x , leading to an δ -independent $\sim L^{1/2}$ effective dynamical exponent at the critical points. The scaling form in Eq. (22) is well verified in the vicinity of the two infinite randomness fixed points, keeping in mind that the control parameter δ is given in Eqs. (17) and (21) for the spin and the orbital Griffiths phases, respectively. We obtain a satisfactory agreement between the numerical results and the analytical calculations in both regions (see Figs. 5 and 6).

2. Correlation length

The correlation length is finite in the Griffiths phase and given either by the average length ξ_J of the spin singlets in the spin Griffiths phase, or by that ξ_t of the orbital singlets in the orbital Griffiths phase. In terms of the appropriate control parameter, given either in Eq. (17) or in Eq. (21), the correlation lengths are divergent in the vicinity of the infinite randomness fixed points, as given in Eq. (9). This relation has been verified by numerical simulations (see Fig. 7), in which—in order to get rid of finite size effects—we used large finite systems with a length up to $L=2048$. For the spin Griffiths phase we used a distribution of the form in Fig. 1(b), whereas for the orbital Griffiths phase the distribution is given in Fig. 1(e). As seen in the figure satisfactory agreement with the theoretical prediction is found, at least for small enough δ and for large L .

V. DISCUSSION AND CONCLUSION

In this paper we have studied the low-energy, low-temperature properties of the one-dimensional Hubbard model in the presence of quenched disorder. Contrary to previous studies⁵⁻⁷ in which disorder was comparatively weak and realized in the form of a random potential, we considered here disorder both in the hopping integrals and in the onsite Coulomb repulsion. Due to the sufficiently strong disorder, the system is always gapless, which means that the low-energy properties are controlled by zero-energy fixed points, for any value of the quantum control parameter. In the framework of the strong disorder renormalization group that we have adapted here to the random Hubbard model, we

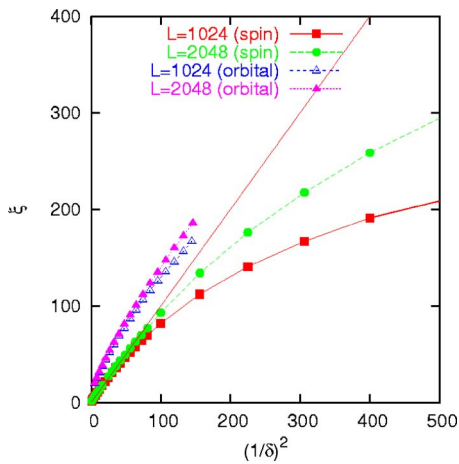


FIG. 7. (Color online) Correlation length in the spin Griffiths phase and the orbital Griffiths phase given by the average length of the spin and orbital singlets, respectively, as a function of the inverse of the square of the control parameter [see Eqs. (17) and (21), respectively]. The theoretical predictions correspond to the solid line $\xi = \delta^{-2}$.

have identified two distinct critical phases, which are controlled by infinite randomness fixed points. For dominant onsite repulsion the system is a spin random singlet infinite randomness phase, whereas for vanishing onsite Coulomb interaction the system corresponds to a random tight-binding model the properties of which are controlled by an orbital infinite randomness fixed point.

The two infinite randomness critical phases are separated by two different Griffiths phases, between which there is a smooth crossover, but no sharp transition. The strong disorder RG method is expected to provide asymptotically exact results close to the critical phases, where the correlation length is divergent. We have made analytical predictions, both for the divergence of the correlation length and that of

the dynamical exponent. These results were compared to large scale numerical RG calculations and satisfactory agreement is found.

To conclude, we mention possible extensions of our work. It is of interest to study the weak-to-strong disorder effects in the random Hubbard chain. For example the charge gap in the Mott insulator phase is expected to be robust against weak disorder, but strong disorder will destroy it, as shown by our RG results. It would also be of interest to study the combined effects of disorder realized at the same time in different parameters (potential, hopping, and interaction). Finally, one may consider extensions of the model to higher dimensions. A different physics is expected already in two dimensions because the interaction dominated phase that maps to a random Heisenberg model has a conventional random fixed point,³³ whereas for vanishing onsite Coulomb repulsion the system is in a logarithmically infinite randomness fixed point.³⁴ However, for a quasi-one dimensional system, made of weakly coupled chains, the transverse exchange couplings of the low energy Heisenberg model are much smaller than the longitudinal ones because of Eq. (6). The one-dimensional spin Griffiths phase due to strong onsite Coulomb interactions is thus expected also in the quasi-one-dimensional system with sufficiently small interchain couplings.

ACKNOWLEDGMENTS

F.I. acknowledges useful discussions with K. Penc and A. Sandvik. This work has been supported by the French-Hungarian cooperation programme Balaton (Ministère des Affaires Etrangères—OM), the Hungarian National Research Fund under Grants Nos. OTKA TO37323, TO48721, K62588, MO45596, and M36803. The Centre de Recherches sur les Très Basses Températures is associated with the Université Joseph Fourier.

¹E. H. Lieb and F. Y. Wu, Phys. Rev. Lett. **20**, 1445 (1968).

²T. Giamarchi and H. J. Schulz, Phys. Rev. B **39**, 4620 (1989); I. Affleck, D. Gepner, H. Shulz, and T. Ziman, J. Phys. A **22**, 511 (1989); R. R. P. Singh, M. E. Fisher, and R. Shankar, Phys. Rev. B **39**, 2562 (1989).

³M. Ogata and H. Shiba, Phys. Rev. B **41**, 2326 (1990).

⁴G. Theodorou and M. H. Cohen, Phys. Rev. Lett. **37**, 1014 (1976).

⁵M. Ma, Phys. Rev. B **26**, 5097 (1982).

⁶A. W. Sandvik and D. J. Scalapino, Phys. Rev. B **47**, 10090 (1993); A. W. Sandvik, D. J. Scalapino, and P. Henelius, *ibid.* **50**, 10474 (1994).

⁷R. V. Pai, A. Punnoose, and R. A. Römer, cond-mat/9704027 (unpublished).

⁸E. Abrahams, P. W. Anderson, D. C. Licciardello, and T. V. Ramakrishnan, Phys. Rev. Lett. **42**, 673 (1979).

⁹S. T. Chui and J. W. Bray, Phys. Rev. B **16**, 1329 (1977); W. Apel and T. M. Rice, *ibid.* **26**, 7063 (1982); Y. Suzumura and H. Fukuyama, J. Phys. Soc. Jpn. **53**, 3918 (1984); T. Giamarchi

and H. J. Schulz, Phys. Rev. B **37**, 325 (1988).

¹⁰L. N. Bulaevskii *et al.*, Zh. Eksp. Teor. Fiz. **62**, 725 (1972) [Sov. Phys. JETP **35**, 384 (1972)]; L. J. Azevedo and W. G. Clark, Phys. Rev. B **16**, 3252 (1977); J. Sanny, G. Grner, and W. G. Clark, Solid State Commun. **35**, 657 (1980); H. M. Bozler, C. M. Gould, and W. G. Clark, Phys. Rev. Lett. **45**, 1303 (1980); L. C. Tippie and W. G. Clark, Phys. Rev. B **23**, 5846 (1981).

¹¹M. Fabrizio and R. Mélin, Phys. Rev. Lett. **78**, 3382 (1997); M. Fabrizio and R. Mélin, Phys. Rev. B **56**, 5996 (1997); M. Fabrizio, R. Mélin, and J. Souletie, Eur. Phys. J. B. **10**, 607 (1999); R. Mélin, *ibid.* **16**, 261 (2000).

¹²S. K. Ma, C. Dasgupta, and C.-K. Hu, Phys. Rev. Lett. **43**, 1434 (1979); C. Dasgupta and S. K. Ma, Phys. Rev. B **22**, 1305 (1980).

¹³For a review of the strong-disorder RG method, see: F. Iglói and C. Monthus, Phys. Rep. **412**, 277 (2005).

¹⁴D. S. Fisher, Phys. Rev. B **50**, 3799 (1994).

¹⁵J. E. Hirsch, Phys. Rev. B **22**, 5355 (1980).

¹⁶K. Biljakovic, M. Miljak, D. Staresinic, J. C. Lasjaunias, P. Mon-

- ceau, H. Berger, and F. Levy, *Europhys. Lett.* **62**, 554 (2003).
- ¹⁷J. Dumas, J. C. Lasjaunias, K. Biljakovic, M. Miljak, H. Berger, and F. Levy, *Solid State Commun.* **132**, 661 (2004).
- ¹⁸S. N. Artemenko and S. V. Remizov, *Phys. Rev. B* **72**, 125118 (2005).
- ¹⁹C. L. Kane and M. P. A. Fisher, *Phys. Rev. Lett.* **68**, 1220 (1992).
- ²⁰E. Altman *et al.*, *Phys. Rev. Lett.* **93**, 150402 (2004).
- ²¹D. S. Fisher, *Phys. Rev. Lett.* **69**, 534 (1992); *Phys. Rev. B* **51**, 6411 (1995).
- ²²P. Henelius and S. M. Girvin, *Phys. Rev. B* **57**, 11457 (1998).
- ²³F. Iglói, R. Juhász, and H. Rieger, *Phys. Rev. B* **61**, 11552 (2000).
- ²⁴K. Hamacher, J. Stolze, and W. Wenzel, *Phys. Rev. Lett.* **89**, 127202 (2002); N. Laflorencie and H. Rieger, *Phys. Rev. Lett.* **91**, 229701 (2003).
- ²⁵R. B. Griffiths, *Phys. Rev. Lett.* **23**, 17 (1969).
- ²⁶P. Wzietek, F. Creuzet, C. Bourbonnais, D. Jérôme, K. Bechgaard, and P. Batail, *J. Phys. (France)* **3**, 171 (1993).
- ²⁷Ch. Krönke, V. Engelmann, and G. Wegner, *Angew. Chem.* **92**, 941 (1980); G. Sachs, E. Dormann, and M. Schwoerer, *Solid State Commun.* **53**, 73 (1985).
- ²⁸R. A. Hyman, K. Yang, R. N. Bhatt, and S. N. Girvin, *Phys. Rev. Lett.* **76**, 839 (1996).
- ²⁹O. Motrunich, K. Damle, and D. A. Huse, *Phys. Rev. B* **65**, 064206 (2002).
- ³⁰R. Mélin, B. Douçot, and F. Iglói, *Phys. Rev. B* **72**, 024205 (2005).
- ³¹K. Damle, *Phys. Rev. B* **66**, 104425 (2002).
- ³²R. Mélin, Y.-C. Lin, P. Lajkó, H. Rieger, and F. Iglói, *Phys. Rev. B* **65**, 104415 (2002).
- ³³Y.-C. Lin, R. Mélin, H. Rieger, and F. Iglói, *Phys. Rev. B* **68**, 024424 (2003).
- ³⁴R. Gade, *Nucl. Phys. B* **398**, 499 (1993); O. Motrunich, K. Damle, and D. A. Huse, *Phys. Rev. B* **65**, 064206 (2002).